CHEMISTRY
A EUROPEAN JOURNAL

FULL PAPER

DOI: 10.1002/chem.201104029

Organocatalytic Kinetic Resolution Cascade Reactions: New Mechanistic and Stereochemical Manifold in Diphenyl Prolinol Silyl Ether Catalysis

Patrick G. McGarraugh,[a] Ryne C. Johnston,[b] Aurora Martínez-Muñoz,[c] Paul Ha-Yeon Cheong,*[b] and Stacey E. Brenner-Moyer*[a]

Abstract: A new cascade reaction involving an iminium-catalyzed intramolecular oxa-Michael addition followed by an enamine-catalyzed intermolecular Michael addition is reported herein. This cascade reaction generates enantiopure, highly functionalized tetrahydropyrans and tetrahydrofurans in a one-pot reaction and in up to 89% combined yield and up to 99% *ee*. This cascade reaction is catalyzed by diaryl prolinol silyl ethers, which are a privileged class of catalysts. The stereochemical outcome of these cascade reactions is unprecedented. Computational studies indicate that this stereochemical outcome arises from nonclassical hydrogen-bonding interactions between the electrophile and the substrate, and from entropic considerations of preorganization. The unprecedented configurations of the cascade products, combined with the computational models, reveal for the first time that asymmetric induction by diaryl prolinol silyl ether catalysts is not always exclusively reagent controlled. The stereochemical outcome also arises from a kinetic resolution or dynamic kinetic resolution of the β-stereocenter through an enamine-catalyzed intermolecular reaction. This unprecedented organocascade reaction mechanism may be adaptable to diaryl prolinol silyl ether-catalyzed cascade reactions, in which both the iminium- and enamine-catalyzed steps are intermolecular, an underdeveloped type of cascade reaction.

Keywords: cascade reactions · domino reactions · kinetic resolution · organocatalysis

Introduction

Since they were first reported in 2005, diaryl prolinol silyl ethers (**1**, Scheme 1) have fast become a privileged class of organocatalysts.[1] While they have proven effective in the production of a diverse array of enantioenriched monofunctionalized saturated aldehydes through enamine or iminium catalysis, arguably their most impressive feat is the catalysis of cascade reactions.[2] Cascade reactions are an efficient green chemical method for rapidly building molecular complexity, in which enamine- and iminium-catalyzed reactions are combined to generate highly functionalized enantiopure aldehydes from simple achiral starting materials in a single flask.

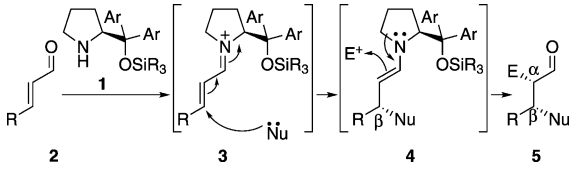

Scheme 1. Model for cascade reactions catalyzed by **1**.

In the most common class of cascade reactions catalyzed by **1**,[3–5] an α,β-unsaturated aldehyde **2** reacts with **1** to form a conjugated iminium ion, **3**. Conjugate addition of a nucleophile (Nu) to **3** occurs from the face opposite the bulky groups of the catalyst. The direct product of this conjugate addition is an enamine, **4**, which can react with an electrophile (E) that approaches from the face opposite the bulky groups of the catalyst. The vast majority of cascade reactions of this type involve nucleophiles that are tethered to electrophiles, rendering the enamine-catalyzed step intramolecular, generating cyclic products. Subsequent hydrolysis of the catalyst reveals a chiral, vicinally functionalized aldehyde, **5**, with the indicated absolute (at the β position) and relative (i.e., α,β-*syn*) configurations. This simple stereochemical model, in which asymmetric induction in reactions catalyzed by **1** is entirely reagent-controlled, rationalizes this stereochemical outcome, which is uniformly observed

[a] P. G. McGarraugh, Prof. S. E. Brenner-Moyer
Department of Chemistry
Brooklyn College of the City University of New York
2900 Bedford Avenue, Brooklyn NY 11210 (USA)
Fax: (+1) 718-951-4607
E-mail: SBrenner@brooklyn.cuny.edu

[b] R. C. Johnston, Prof. P. H.-Y. Cheong
Department of Chemistry
Oregon State University
153 Gilbert Hall, Corvallis, OR 97331 (USA)
Fax: (+1) 541-737-2062
E-mail: paulc@science.oregonstate.edu

[c] A. Martínez-Muñoz
Departmento de Química Orgánica
Universidad de Sevilla
41012 Sevilla (Spain)

Supporting information for this article is available on the WWW under http://dx.doi.org/10.1002/chem.201104029.

regardless of the nature of the nucleophile and electrophile, or whether they are tethered or untethered.[3–5]

We recently began investigating the cascade reaction illustrated in Scheme 2.[6] We were interested in this cascade reaction for several reasons. First, it would entail a novel oxa-Michael addition (**8**→**9**). Second, it would be a rare example of a cascade reaction catalyzed by **1** in which the nucleophile (i.e., OH) and electrophile (E) are untethered. Finally, it would generate both 2,5-*cis*- *and trans*-tetrahydrofurans (**10**, $n=1$) and 2,6-*cis*- and *trans*-tetrahydropyrans (**10**, $n=2$), all of which are prevalent substructures in bioactive complex natural products.

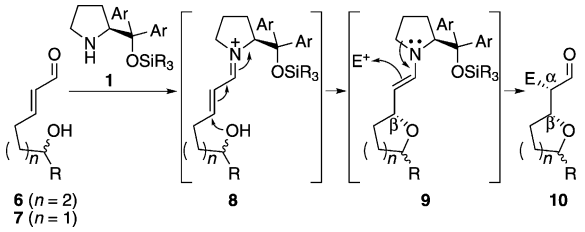

Scheme 2. Proposed cascade reaction.

During the course of these investigations, we observed a dramatic difference in the behavior of substrates of type **6** and that of substrates of type **7** in both steps of this cascade reaction. Additionally, *none* of the cascade products arising from either **6** or **7** had the expected absolute (at the β position) and relative (i.e., α,β-*syn*) configurations that are typical of cascade products generated using **1** (i.e., those of **10**). These results, presented herein, provide new insight into the stereochemical and mechanistic models for cascade reactions employing this popular class of organocatalysts.

Results and Discussion

Oxa-Michael addition of tetrahydropyran-forming substrates: In the presence of catalyst **1**, racemic substrates of type **6a** undergo an intramolecular oxa-Michael addition via iminium **11** (Scheme 3). Conjugate addition of the hydroxyl group from the face opposite the bulky groups of the catalyst directly produces enamine **12**, which, upon hydrolysis, yields *cis*- and *trans*-tetrahydropyran products, **13**-*cis* and **13**-*trans*. These products were initially formed in an approximately 1:1 ratio, and in good (in the case of the *cis*-product) to excellent (in the case of the *trans*-product) selectivities. There was, however, a strong thermodynamic preference for the (all-equatorial) *cis*-product. This led to rapid epimerization of **13**-*trans* at the β position, thereby generating *ent*-**13**-*cis*, which increased the *cis*/*trans* ratio while decreasing the *ee* of **13**-*cis*.

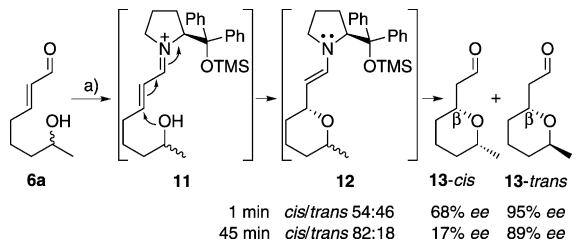

Scheme 3. Oxa-Michael addition of tetrahydropyran-forming substrates. a) **6a**, **1** (10 mol%), $PhCO_2H$ (10 mol%), toluene (0.4 M), 0 °C.

Cascade reaction with tetrahydropyran-forming substrates: In the presence of catalyst **1** and β-nitrostyrene as an external electrophile, a kinetic resolution of racemic substrates **6** resulted (Scheme 4). Substrates **6** underwent an oxa-Michael addition, initially forming **13**-*cis* and -*trans*. The latter rapidly epimerized to *ent*-**13**-*cis*, thereby generating a racemic mixture of *cis*-tetrahydropyrans, *rac*-**13**-*cis*. One enantiomer, *ent*-**13**-*cis*, underwent a subsequent enamine-catalyzed Michael addition to β-nitrostyrene to produce, after reduction, cascade product **15**. The rate of this reaction of the other enantiomer, **13**-*cis*, was substantially diminished, and **13**-*cis* was largely recovered (as **14**, after reduction).

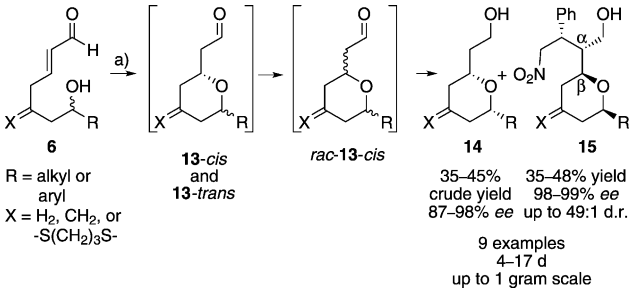

Scheme 4. Organocascade kinetic resolution. a) **6** (0.44 mmol), β-nitrostyrene (0.88 mmol), **1** (0.088 mmol), $PhCO_2H$ (0.088 mmol), toluene (1.1 mL), −30 °C, then THF·BH_3 (1 M in THF, 0.5 mL) or $NaBH_4$ (2 mmol), MeOH (4.4 mL).

This was, in fact, a rare example of a kinetic resolution by enamine catalysis.[6] Moreover, the resolved intermediates are useful synthons; one was readily transformed in ≤ three steps into known intermediates in the total synthesis of (−)-dactylolide and leucascandrolide A.[6]

Arguably more notable than the kinetic resolution is the stereochemical outcome of this transformation. The absolute (at the β position) and relative (at the α vs. β positions) configurations of the cascade products **15** were opposite those that normally arise from use of catalyst **1** (i.e., **15** vs. **5**). This unprecedented stereochemical outcome can be accounted for by the proposed stereochemical and mechanistic models for this kinetic resolution, discussed in later sections.

This methodology was also compatible with other β-nitrostyrene substrates, including electron-rich and -poor β-nitrostyrenes (Scheme 5). Use of diethylazodicarboxylate or nitrosobenzene as alternative electrophiles in this kinetic resolution, however, was not successful. This may be because these electrophiles lack suitably acidic hydrogens that can

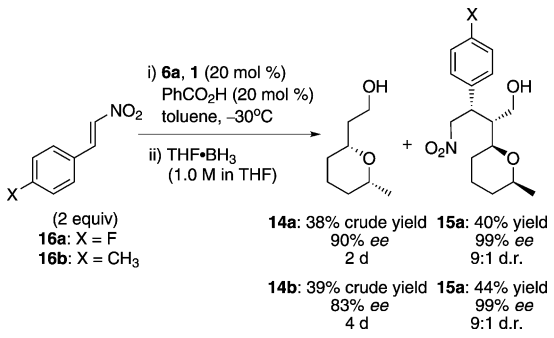

Scheme 5. Other β-nitrostyrene substrates.

participate in nonclassical hydrogen-bonding interactions (see below).

Although a variety of substrates were tolerated in this kinetic resolution, several substrates were not successfully resolved under these conditions (Figure 1). These included substrates with sterically less demanding R groups, such as **6b** and **6c**, which contain sp^2- and sp-hybridized carbons, respectively, directly bound to the resulting tetrahydropyran ring. For these substrates, the *trans*-tetrahydropyran oxa-Michael adduct (**13**-*trans*) persisted, likely due to the reduced thermodynamic preference for the (all-equatorial) *cis*-tetrahydropyran. Multiple cascade products were also observed, several of which presumably arose from the *trans*-tetrahydropyran oxa-Michael adduct.

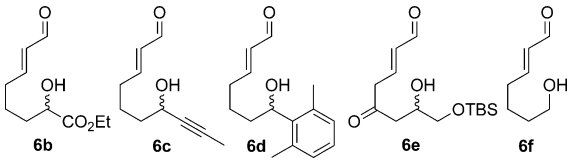

Figure 1. Other substrates for the organocascade kinetic resolution.

Substrates **6d** and **6e**[7] formed one predominant cascade product, and the reactions were quenched when a good crude yield of this cascade product **17** and of the oxa-Michael adduct **13**-*cis* was achieved and when their ratio was approximately 1:1 (Scheme 6). For all substrates in Scheme 4, this led to high *ee* values of both the cascade product and of the oxa-Michael adduct. For substrates **6d** and **6e**, the cascade reaction was exceedingly sluggish (13–35 d) and **13**-*cis* was recovered (as its corresponding alcohol) in low *ee*. While all substrates of type **13** can epimerize at the 2-, or β position (as in the conversion of **13**-*trans* to *ent*-**13**-*cis*), only **13d** and **13e** have a mechanism by which they can also epimerize at the 6-position. Substrate **13d**-*cis* can form a benzylic cation stabilized through resonance with the electron-rich benzene ring. Substrate **13e**-*cis* can undergo a β-alkoxide elimination to form an enone, which could be facilitated by deprotonation of the indicated acidic protons by the secondary amine catalyst. We therefore believe that these two substrates were slowly undergoing a dynamic kinetic resolution; **13**-*cis* was slowly converting to *ent*-**13**-*cis*,

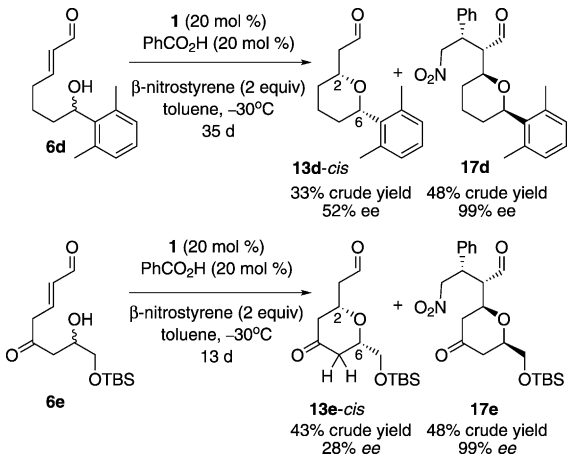

Scheme 6. An organocascade dynamic kinetic resolution.

which (even more slowly) went on to ultimately produce **17**, although it should be noted that we did not allow complete consumption of **13**-*cis* to test this hypothesis.

Finally, substrate **6f**, without an R group, formed two cascade products, **18** and **15f**, arising from Michael addition of both enantiomers of *rac*-**13f** to β-nitrostyrene (Scheme 7). This result demonstrated that, for the tetrahydropyran-forming substrates, the R group is necessary for the kinetic resolution of oxa-Michael adducts, *rac*-**13**-*cis*.

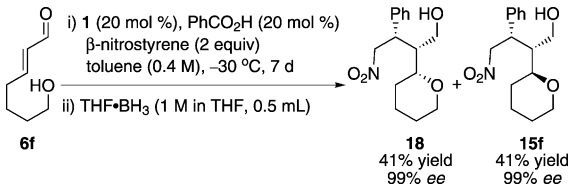

Scheme 7. R group controls outcome of enamine-catalyzed Michael addition.

Oxa-Michael addition of tetrahydrofuran-forming substrates: In the presence of catalyst **1**, racemic substrates of type **7a** also undergo an intramolecular oxa-Michael addition (Scheme 8). As in the case of tetrahydropyran-forming

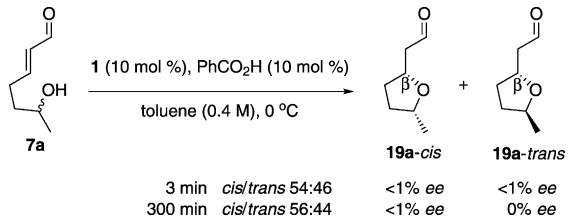

Scheme 8. Oxa-Michael addition of tetrahydrofuran-forming substrates.

substrate **6a**, this addition appears to be iminium-catalyzed, as it does not occur on this time scale in the absence of catalyst, nor in the presence of base (Et_3N) or acid ($PhCO_2H$) alone. Also like the tetrahydropyran-forming substrates, *cis*- and *trans*-tetrahydrofuran products, **19a**-*cis* and -*trans*, are

initially formed in an approximately 1:1 ratio. Unlike the tetrahydropyran-forming substrates, however, both the *cis*- and *trans*-tetrahydrofuran products are formed completely nonselectively, in <1% *ee*. Moreover, the approximately 1:1 *cis*/*trans* ratio persists over time, possibly due to the reduced thermodynamic preference for a configuration that enables an all-(pseudo)equatorial conformation.

Cascade reaction with tetrahydrofuran-forming substrates: In the presence of catalyst **1** and β-nitrostyrene (**16c**) as an external electrophile, cascade products, **20a**-*cis* and **20a**-*trans*, with *cis*- and *trans*-tetrahydrofuran rings, respectively, were generated (Scheme 9). This was not entirely surprising

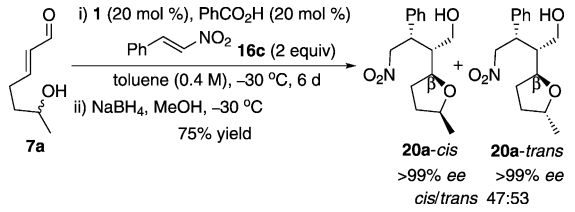

Scheme 9. Cascade reaction with tetrahydrofuran-forming substrates.

in light of the fact that, as discussed in the preceding section, both *cis*- and *trans*-tetrahydrofuran rings (i.e., **19a**-*cis* and **19a**-*trans*) arose from, and persisted in, the iminium-catalyzed oxa-Michael addition. What was surprising, however, was that while racemic *cis*- and *trans*-tetrahydrofuran rings arose from the iminium-catalyzed oxa-Michael addition, the subsequent enamine-catalyzed Michael addition to β-nitrostyrene generated *cis*- and *trans*-tetrahydrofuran ring-containing cascade products in >99% *ee*.

This is indicative of a dynamic kinetic resolution of the β-stereocenter (Scheme 10). Oxa-Michael adducts, **19a**-*cis* and -*trans*, with *R* configuration at the β position (i.e., **19a** (*R*)), can react with the catalyst to generate enamine **21**, which evidently does not react with β-nitrostyrene (**16c**). Instead, a retro-oxa-Michael addition followed by a forward oxa-Michael addition, to epimerize the β position of either oxa-Michael adduct **19a** (*R*) (to form **19a** (*S*)) or of enamine **21** (to form **23**), occurs. Oxa-Michael adducts **19a**-*cis* and -*trans*, with *R* configuration at the β position, would thereby ultimately be converted to enamine **23**, with *S* configuration at the β position, which does react with β-nitrostyrene, and which can alternatively form directly from reaction of the catalyst with *ent*-**19a**-*cis* and -*trans* (i.e., **19** (*S*)).

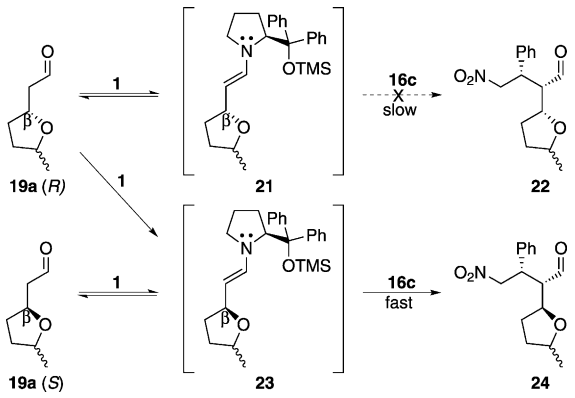

Scheme 10. Dynamic kinetic resolution with respect to configuration at β position.

As indicated in Scheme 11, a variety of substrates afforded similar outcomes to that of **7a** in this cascade, including alcohols with adjacent sterically demanding alkyl substituents (**7d**), silyl protecting groups (**7f**), sp^2-hybridized carbons (**7g**, **7h**), and stereocenters (**7i**, **7j**), as well as substrates containing other reactive functional groups (**7e**). More specifically, in all cases, cascade products **20**-*cis* and **20**-*trans*, with *cis*- and *trans*-tetrahydrofuran rings, respectively, were generated in >95% *ee* and in an approximately 1:1 ratio. Interestingly, there was a slight preference for the *trans*-tetrahydrofuran cascade products in all cases, which contrasts with the initial oxa-Michael addition that slightly favored formation of the *cis*-tetrahydrofuran (Scheme 8).

In substrates **20i** and **20j**, the presence of the additional, adjacent stereocenter did impact the outcome of the cascade reaction. While the *cis*/*trans* ratio did not change or changed only modestly, the d.r. of the *cis*- and *trans*-products changed dramatically. Compounds **20i**-*cis* and **20j**-*cis* formed without diastereoselectivity, while **20i**-*trans* and **20j**-*trans* were formed in outstanding d.r. Additionally, an oxepane-forming substrate readily decomposed under these reaction conditions.

The configuration of cascade products **20a**-*cis* and **20a**-*trans* at the 5-position was established by running the cascade reaction with the pure *R* and pure *S* enantiomers of substrate **7a**. The remaining stereocenters in **20a**-*cis* and **20a**-*trans* were established by X-ray crystallography.[8] The stereochemistry of all other cascade products of type **20** was assigned by analogy.

As with the tetrahydropyran-containing cascade products, **15**, all tetrahydrofuran-containing cascade products, **20**, contain absolute (β position) and relative (α vs. β positions) configurations that are opposite those that normally arise from use of catalyst **1** (i.e., **20** vs. **5**). This unprecedented stereochemical outcome can be accounted for by the proposed stereochemical and mechanistic models for this cascade reaction, discussed in the next two sections.

Unlike the tetrahydropyran-forming substrates, **6**, the R group in the tetrahydrofuran-forming substrates, **7**, did not influence the reactivity of the oxa-Michael adducts in the enamine-catalyzed Michael addition to β-nitrostyrene. Evidence in support of this is the formation of cascade products (**20a–j**) with both *R* and *S* configurations at the 5-position. All cascade products do, however, have the same configuration at the β position. This suggests that, in contrast to substrates of type **6**, it is the configuration at the β position that dictates the reactivity of the oxa-Michael adducts arising from substrates **7** in the enamine-catalyzed Michael addition to β-nitrostyrene. Further evidence in support of this is that

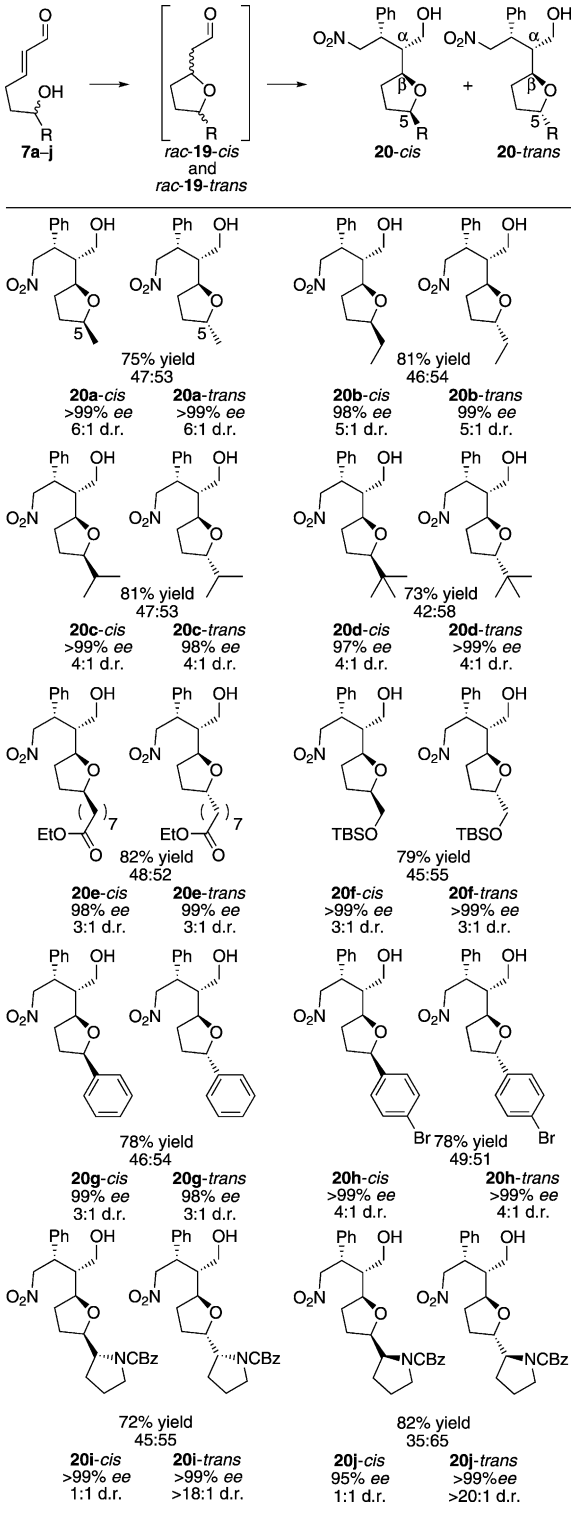

Scheme 11. Scope of cascade reaction with tetrahydrofuran-forming substrates.[a–e] a) **7** (0.44 mmol), **16c** (0.88 mmol), **1** (0.088 mmol), $PhCO_2H$ (0.088 mmol), toluene (1.1 mL), −30 °C, then $NaBH_4$ (2 mmol), MeOH (4.4 mL), −30 °C. b) Yield = combined isolated yield of **20**-*cis* and -*trans*. c) d.r. of the **20**-*cis* and -*trans* products was determined by ^{1}H NMR spectroscopy and is defined as the ratio of the amount of the major cascade product to the sum of the amounts of the minor cascade products, usually three, arising from the *R* and *S* enantiomers, respectively, of **7**. d) *ee* values of alcohol determined by chiral phase HPLC. e) All reaction times were 6 d.

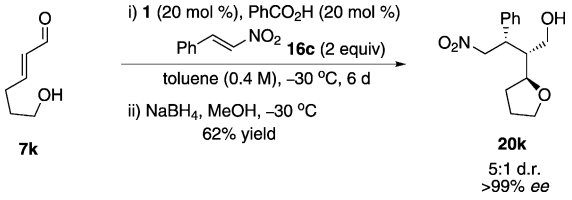

Scheme 12. β-Group, not R group, controls outcome of enamine-catalyzed Michael addition.

substrate **7k**, without an R group, forms a single cascade product (Scheme 12).

Proposed model for stereochemical outcome of cascade reactions: All cascade products generated in these studies (**15** and **20**) possess *S* configuration at the β position. This configuration effectively arises from the approach of the alcohol from the *same* face as the bulky groups of the catalyst in the initial iminium-catalyzed oxa-Michael addition. As mentioned, this is not typically observed in reactions catalyzed by **1**, and results in cascade products with unprecedented absolute (at the β position) and relative (α vs. β positions) configurations.

With the current understanding of the selectivities of reactions catalyzed by **1**, such stereochemical outcomes could only arise if the second step (Michael addition to β-nitrostyrene) was rate- and stereodetermining. The former supposition is supported by experimental data: in all cases, the oxa-Michael addition was observed by ^{1}H NMR to be complete within 12 h, while a further 2–35 d was required for completion of the Michael addition to β-nitrostyrene. Transition states (TSs) of the carbon–carbon bond-forming event involving β-nitrostyrene and the catalyst-enamine of substrates **6a** (**TS-IV**), **6f** (**TS-II**), **7a** (**TS-III**), and **7k** (**TS-I**) were, therefore, computed in order to quantify the stereocontrolling elements. Exhaustive DFT conformational searches of the C–C bond-forming transition states were performed. Structures and thermodynamic corrections were computed using B3LYP/6-31G* in toluene (PCM), as implemented in the Gaussian 09 suite of programs. Energies were refined using SCS-MP2/cc-pVTZ, as implemented in the Q-Chem 4.0.[9] Although the ubiquitous B3LYP/6-31G* often overestimates activation barriers and reaction endergonicity due to poor treatment of dispersion interactions, we at Oregon State have recently discovered that SCS-MP2 single point energies correct for the lack of dispersion in B3LYP/6-31G* results, leading to a remarkable accuracy in barrier heights and stereoselectivities where other methods have failed.[10]

The lowest energy conformations of the transition states for the Michael addition to β-nitrostyrene are shown for each stereoisomer in Figure 2.[11] The *R* or *S* labels refer to the stereochemistry at the β position of the enamine substrate. All transition-state conformations are remarkably similar, with forming C–C bond lengths around 2.1 Å. Although the orientations of the catalyst side chain vary between the different transition states, the energetic differen-

ces between these conformations are small, around 0.5 kcal mol^{-1}.[12b] The lowest energy conformations have the developing bond between the enamine and β-nitrostyrene occurring from the sterically accessible face of the enamine, opposite the bulky groups of the catalyst side chain. Additionally, the conformation around the β-stereocenters is such that it minimizes the steric and torsional interactions with the approaching β-nitrostyrene electrophile.

There is good agreement between the computed selectivities and experiments. DFT geometry optimizations in solvent (toluene) in conjunction with SCS-MP2 energetics was critical in reproducing the stereoselectivity trends, namely, that the **TS-I**, **TS-III**, and **TS-IV** series are much more selective than **TS-II**. B3LYP gas-phase results erroneously predict that **TS-II** is the most selective (>2 kcal mol^{-1}), and geometry optimizations in solvent erroneously predict the same level of stereoselectivity for **TS-II** and **TS-IV** ($\Delta\Delta G^{\ddagger}=$ 1.2 kcal mol^{-1}), in disagreement with experiments that showed no selectivity for the TS-II series ($\Delta\Delta G^{\ddagger}=0.0$ kcal mol^{-1}).

The stereoselectivity of the Michael addition to β-nitrostyrene is controlled by three factors: a) the *anti* versus *syn* catalyst-enamine preference; b) the *Re* or *Si* facial selectivity of the nitrostyrene electrophile; and c) the effect of the stereochemistry of the β position of the enamine substrate. Prolinol catalysts are known to favor the *anti*-orientation of

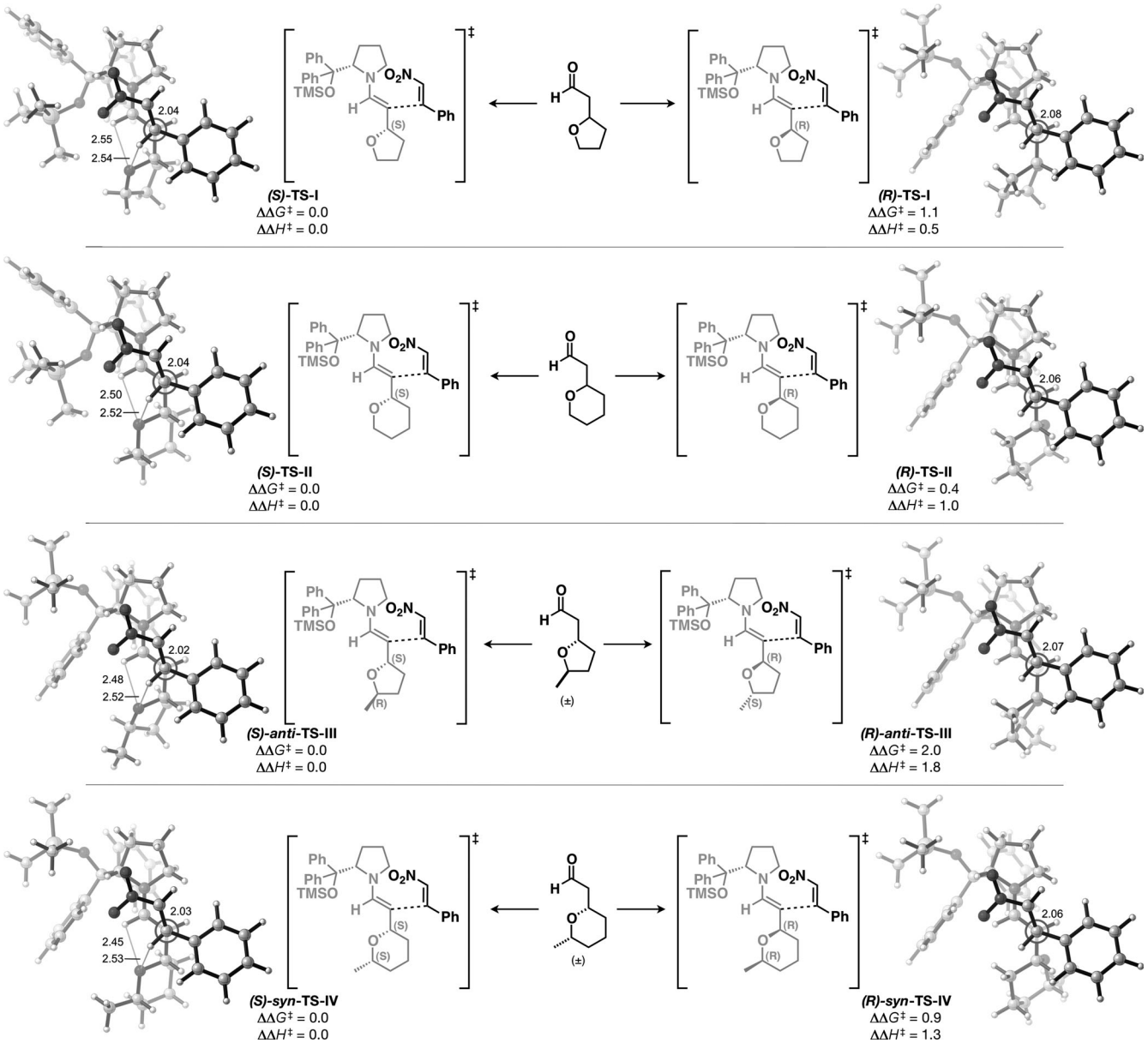

Figure 2. C–C Bond-forming transition structures between β-nitrostyrene and the catalyst–enamine of substrates **6a** (**TS-IV**), **6f** (**TS-II**), **7a** (**TS-III**), and **7k** (**TS-I**). Experimentally, substrates **6a**, **7a**, and **7k** show greater selectivity than **6f**, and the computed results are consistent in that they show that the **TS-I**, **TS-III**, and **TS-IV** are much more selective than the **TS-II** series.

the nucleophilic double bond with respect to the catalyst side chain, both in the enamine ground state and the Michael transition states.[12] The nitrostyrene facial selectivity is governed by electrostatic contact between the developing negative charge of the nitro group and the developing positive charge of the enamine in the Michael transition state.[1b] The *Si* face attack guarantees maximal electrostatic contact and stabilization, and therefore is favored. In all cases, the shortest distance between the nitro group and the enamine nitrogen is >3 Å, indicating nonbonding interaction is in effect, rather than covalent.

While the first two factors are well understood, the effect of the stereochemistry of the β position of the enamine substrate is poorly understood. Initially, in seeking an explanation for this unprecedented stereochemical outcome, we proposed that this might result from differential shielding of enamine faces by the β-stereocenter in the enamine-catalyzed Michael addition to β-nitrostyrene.[6] However, DFT (B3LYP/6-31G*) modeling of various enamine intermediates revealed no pronounced facial discrimination of the catalyst enamines arising from the β-stereocenter.

The examination of the computed nitrostyrene transition structures reveals that the β-stereocenter of the catalyst–enamine controls the stereoselectivity in two ways: a) enthalpic stabilization from nonclassical hydrogen bonds and b) entropic penalty from preorganization of the reactants in the transition states.

Enthalpic stabilization of (S)-TSs from nonclassical hydrogen bonds: Energetically, at least half of the stereocontrol arises from stabilizing nonclassical hydrogen bonds (electrostatic contacts) between the heterocycle of the catalyst-enamine and the incoming electrophile. Specifically, the (*S*)-TSs are stabilized through nonclassical hydrogen bonds between the approaching β-nitrostyrene benzylic hydrogen and the oxygen of the enamine heterocycle (distances ca. 2.5 Å, indicated by thin lines, Figure 2).[13] In the disfavored (*R*)-TSs, this stabilizing electrostatic contact is replaced by a repulsive electrostatic interaction between a methylene and the β-nitrostyrene benzylic hydrogen. This enthalpic preference is worth 0.5 and 1 kcal mol^{-1} for unsubstituted furan and pyran substrates (**TS-I** and **TS-II**), respectively. However, inclusion of the methyl group (**TS-III** and **TS-IV**) slightly increases the selectivity, possibly through inductive effects that strengthen the basicity of the heterocycle oxygen.

Entropic penalty of preorganization: Entropic penalties accompany preorganization. In this particular study, we have discovered that the entropic considerations play a significant role in determining the stereoselectivity.

In unsubstituted pyrans (**TS-II**), the enthalpic preference ($\Delta\Delta H^{\ddagger}$) for the (*S*)-TS over the (*R*) is 1.0 kcal mol^{-1}. However, the conformational preorganization that arises from the nonclassical hydrogen bonds in the (*S*)-TS is entropically disfavored. Therefore, the free energy preference ($\Delta\Delta G^{\ddagger}$) is smaller in magnitude compared to the enthalpic preference, to the tune of 0.4 kcal mol^{-1}. This entropic penalty is halved in the methyl-substituted case (**TS-IV**) because the equatorial preference of the methyl diminishes the entropic penalty for conformational preorganization of the pyran. This leads to a scenario in which the enthalpic and free energy selectivity are much more similar ($\Delta\Delta H^{\ddagger}=1.3$ and $\Delta\Delta G^{\ddagger}=0.9$ kcal mol^{-1}).

In unsubstituted (**TS-I**) and methyl-substituted (**TS-III**) furans, the opposite scenario occurs - the free energy preference ($\Delta\Delta G^{\ddagger}$) of (*S*)-TSs over *(R)* is greater than the enthalpic preference ($\Delta\Delta H^{\ddagger}$). For an example, in **TS-I**, the $\Delta\Delta H^{\ddagger}$ is 0.5 kcal mol^{-1}, while the free energy preference is 1.1 kcal mol^{-1}. This heightened free energy preference signifies that the (*R*)-TS is conformationally more rigid (preorganized) than the (*S*)-TS. This is due to an enthalpic stereoelectronic preference for the furan C–O bond to be *anti*-periplanar to the forming C–C bond with the incoming electrophile (*anti*-periplanar atoms circled in Figure 3). Only in the (*R*)-TS, can this *anti*-periplanar arrangement of a C–O bond with respect to the forming C–C bond be realized, leading to transition state preorganization and thus entropic penalty. In the (*S*)-TS, the forming C–C bond is *anti*-periplanar to a ring C–C bond, an arrangement with much weaker electronic bias and therefore weaker entropic penalization. Interestingly, this *anti*-periplanar arrangement between the forming C–C bond and the heterocycle C–O bond only occurs for the (*R*)-TS of furans (**TS-I** and **TS-III**), but not the pyrans (**TS-II** and **TS-IV**). In the furan series, this arrangement is clearly *anti* (~177°), while in the pyran series, it is not (~165°), as shown in Figure 3. This explains why the entropic enhancement of selectivity only occurs in the furan series.

Earlier this year, the Blackmond and Armstrong groups published a seminal mechanistic study of **1**-catalyzed enamine-mediated conjugate addition of achiral aldehydes to β-nitrostyrene.[14] In this report, they found that the resting state of the catalyst was a cyclobutane intermediate arising from the condensation of the nitroenolate and the catalyst iminium immediately following the Michael addition. Although we cannot rule out a role for analogous cyclobutane species or other stable downstream intermediates in the stereo-determining step, the currently available experimental and computational data are consistent with the hypothesis that the carbon-carbon bond forming step is stereodetermining.

This proposed model accounts for the selectivities of all substrates examined experimentally. Importantly, the unprecedented stereochemical outcome of these **1**-catalyzed cascade reactions combined with the proposed enthalpic and entropic stereocontrolling elements that rationalize this outcome together suggest that the accepted stereochemical model for asymmetric induction in reactions catalyzed by **1** as being entirely reagent-controlled is an oversimplification. Evidently, there is a more complex relationship between the role of the substrate and that of the catalyst in asymmetric induction in reactions catalyzed by **1** than has previously been suggested.

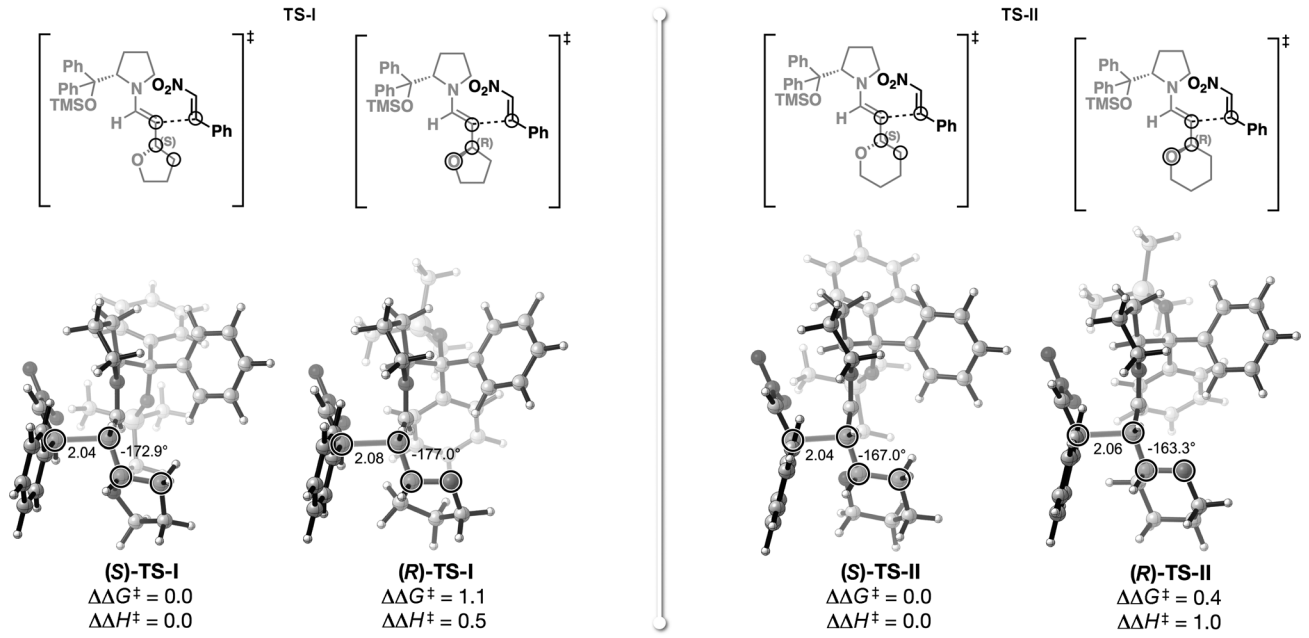

Figure 3. Side views of the C–C bond-forming transition structures between β-nitrostyrene and the catalyst–enamine of substrates **6f** (**TS-II**) and **7k** (**TS-I**) shown in Figure 2. In the furan series, for an example the **TS-I** series, the C–O bond of the heterocycle is antiperiplanar to the forming C–C bond, while in the pyran series, for an example the **TS-II** series, it is not. The four atoms involved in this relationship are circled, and the associated dihedral angles reveal that the **TS-I** transition structures are *anti* (≈177°), whereas the analogous angles in **TS-II** transition structures are not (≈165°).

Proposed mechanistic model of cascade reactions: The proposed mechanistic model for these cascade reactions is illustrated in Scheme 13. As discussed previously, the initial oxa-Michael addition is reversible and ultimately generates racemic oxa-Michael adducts **25** (*cis* only for $n=2$, *cis* and *trans* for $n=1$). Oxa-Michael adducts possessing *S* configuration at the β-carbon react with the catalyst to form enamine **26**, while those possessing *R* configuration at the β-carbon react with the catalyst to form enamine **9**.

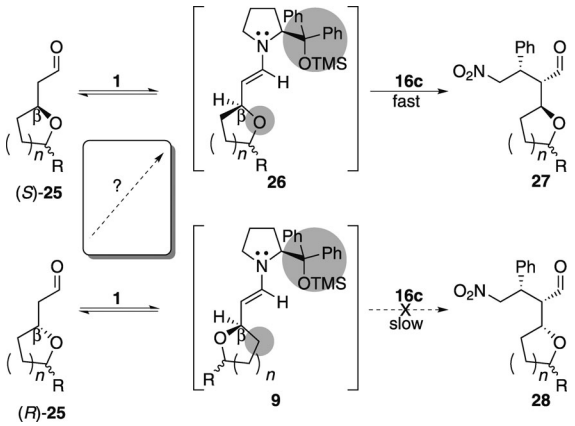

Scheme 13. Proposed mechanistic model.

As discussed in the preceding section, synergism between the blocking effects of the catalyst side chain and the directing effects of the nonclassical hydrogen-bond capabilities of the substrate in enamine **26**, in conjunction with relatively favorable entropic considerations, result in a relatively rapid reaction with an electrophile that approaches from the back face of the enamine, generating cascade products of type **27**. Entropic penalties and/or the absence of this synergism in enamine **9**, account for its relative unreactivity and for the observation of, in most cases, only trace formation of cascade products of type **28**.

If a retro-oxa-Michael addition/forward oxa-Michael addition to epimerize (*R*)-**25** or **9** at the β position can occur, then a dynamic kinetic resolution of the β-stereocenter is possible. This occurs with all tetrahydrofuran-forming substrates (**25**, $n=1$), and both (*S*)-**25** and (*R*)-**25** generate cascade products of type **27**, with the *S* configuration at the β position. As mentioned, we also suspect this occurs with tetrahydropyran-forming substrates **6d** and **6e**.

If a retro-oxa-Michael addition/forward oxa-Michael addition to epimerize (*R*)-**25** or **9** at the β position is not possible, then a kinetic resolution occurs. This occurs with the tetrahydropyran-forming substrates (**25**, $n=2$), because epimerization of enamine **9a** (or its corresponding aldehyde) at the β position would generate a thermodynamically disfavored *trans*-tetrahydropyran ring, **26a**, in which one of the substituents on the ring must occupy an axial position (Scheme 14). Thus, for tetrahydropyran-forming substrates, enamine **26** produces a cascade product, **27**, whereas enamine **9** cannot readily convert to cascade product **28** nor to enamine **26**, and so simply reverts back to (*R*)-**25**.

This mechanistic model accounts for the different reactivity of the tetrahydropyran- and -furan-forming substrates. It also presents an interesting possibility. A general strategy to obtain products with high selectivity in cascade reactions ini-

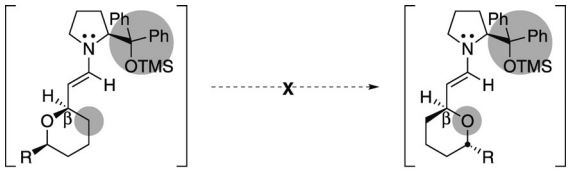

Scheme 14. Epimerization at β position generates the *trans*-tetrahydropyran ring.

tiated by reversible iminium-catalyzed conjugate additions has been to compensate for the reversible conjugate addition to prevent racemization of conjugate addition products at the β position. This has most often been done using an enamine-catalyzed intramolecular reaction. As a result, as mentioned earlier, the vast majority of cascade reactions catalyzed by **1** employ nucleophiles tethered to electrophilic centers, forming cyclic products. In so doing, a reversible iminium-catalyzed conjugate addition can be compensated for via: A) an intramolecular enamine-catalyzed reaction that is more rapid than the retro-conjugate addition reaction, or B) a dynamic kinetic resolution of the β-stereocenter of racemic conjugate addition products via an intramolecular enamine-catalyzed reaction. Our data reveals for the first time that the latter scenario is also possible through intermolecular enamine-catalyzed reactions. Thus, using appropriately chosen untethered nucleophiles and electrophiles, it may be possible to develop cascade reactions, in which both steps are intermolecular, and which take advantage of the reversibility of iminium-catalyzed conjugate additions to obtain cascade products with high selectivity through a dynamic kinetic resolution process. Cascade reactions of this type would generate enantiopure, highly functionalized acyclic products, possibly with configurations analogous to those reported herein. Moreover, cascade reactions of this type would lead to an expansion of the limited scope of cascade reactions catalyzed by **1** in which both the iminium- and enamine-catalyzed steps are intermolecular.

Conclusion

In summary, we have developed novel cascade reactions that lead to enantiopure tetrahydropyran and tetrahydrofuran substrates. Notably, all of the cascade products manifest unusual, unprecedented stereochemical configurations opposite of what has been previously reported for diphenyl prolinol silyl ether catalysts. This observation, in conjunction with computational studies, is evidence of a more complex relationship between the role of the substrate and that of the catalyst in asymmetric induction in reactions catalyzed by this privileged class of catalysts than has previously been disclosed. The mechanistic implications of the cascade reactions discussed herein may be amenable to other cascade reactions involving an intermolecular enamine-catalyzed step. This may aid in the development of cascade reactions catalyzed by **1** in which both the iminium- and enamine-mediated steps are intermolecular, a class of cascade reactions that has thus far been considerably limited in scope.

Experimental Section

General information: All chemicals and solvents were purchased from Sigma–Aldrich, Fisher Scientific or VWR International. ^{1}H and ^{13}C NMR spectra were collected using a Bruker 400 MHz Biospin. The NMR data herein uses the following abbreviations: s = singlet, d = doublet, t = triplet, q = quartet, m = multiplet, dd = doublet of doublets, td = triplet of doublets, dt = doublet of triplets, ddt = doublet of doublet of triplets. Enantiomeric excesses were determined using a Perkin–Elmer Series 200 HPLC with Daicel Chemical Industries, LTD. Chiralpak AD-H (0.46×25 cm), Chiralpak OD-H (0.46×25 cm), and Chiralpak AS-H (0.46×25 cm) columns. Enantiomeric excesses were determined by comparison to a racemic sample (prepared with the corresponding racemic catalyst). Optical rotations were determined using a Jasco P-1020 polarimeter. IR spectra were collected using a Nicolet 6700 FT-IR. High resolution mass spectra were collected using an Agilent 6520 Q-TOF. Flash chromatography was carried out with Merck, grade 9385, 230–400 mesh, 600 Å silica gel and with Merck, silica 60F-254 on glass, 250 μm layer TLC plates with fluorescent indicator. Solvents were dried and kept air free in a solvent purification unit. Solvents were evaporated using a standard rotovapor and a high vacuum. All reactions were carried out in oven dried glassware and conducted under an argon atmosphere. In all cases, yield refers to an isolated yield, unless otherwise indicated.

Characterization and supporting information for previously published compounds: Full characterization of compounds of type **6**, **14** and **15** (Scheme 4) as well as copies of ^{1}H NMR spectra, ^{13}C NMR spectra, and HPLC chromatograms is contained in the Supporting Information for reference [6].

General procedure for the organocascade reaction of pyrans and furans: Catalyst **1** (28.6 mg, 0.088 mmol) and $PhCO_2H$ (10.7 mg, 0.088 mmol) were dissolved in dry toluene (1.1 mL) and cooled to −30 °C. Substrate **6** or **7** (0.44 mmol) was added in one portion. Compound **16** (131.2 mg, 0.88 mmol) was added after 5 min and the reaction was stirred at −30 °C. The reaction was monitored by ^{1}H NMR. (Note: for the furan forming reactions, *two* identical reactions were setup.)

For the pyran reactions (14, 15 and 18): Once the resolution was judged to be complete (the corresponding aldehyde of **14** and the corresponding aldehyde of **15** are present in the reaction mixture in roughly equal amounts, as determined by ^{1}H NMR of the reaction mixture), the crude yield of **14** was determined by ^{1}H NMR of the crude reaction mixture using an internal standard. The d.r. of **15** was also determined by ^{1}H NMR of the crude reaction mixture. The d.r. of **15** was calculated by integration of the aldehyde peaks of all diastereomers of the corresponding aldehyde of **15** resulting from the *S* enantiomer of **6**. An in situ reduction was performed using conditions A or B below.

***Reduction conditions A**:* For reactions with substrates **6a**, **6d**, and **6f**, $BH_3{\cdot}THF$ (1.0 M in THF, 0.50 mL) was added dropwise to the reaction mixture and the reaction was allowed to warm to 0 °C over 30 min. The reaction was quenched by adding 1.0 M aqueous HCl (4 mL). The aqueous layer was extracted with CH_2Cl_2 (2×15 mL). The combined organic layers were dried over $MgSO_4$, filtered and concentrated.

***Reduction conditions B**:* For reaction with substrate **6e** the reaction mixture was diluted with MeOH (4.4 mL), and $NaBH_4$ (75.7 mg, 2.0 mmol) was added. The reaction was stirred at −30 °C for 15 min and was quenched by slowly adding saturated aqueous NH_4Cl (5 mL). The aqueous layer was extracted with CH_2Cl_2 (2×15 mL). The combined organic layers were dried over $MgSO_4$, filtered and concentrated.

Both oxa-Michael product **14** and cascade product **15** were purified from the residue by column chromatography (EtOAc/petroleum ether 30:70).

For the furan reactions (20a–j *cis* and *trans*, and 20k): Upon complete conversion to the *cis* and *trans* cascade products, one of the two reactions was reduced using Reduction conditions B. Products **20**-*cis* and **20**-*trans*

were purified from the residue by column chromatography (EtOAc/CH_2Cl_2 2:98) and an isolated yield was determined. The major **20**-*cis* diastereomer was isolated in this way. The major **20**-*trans* diastereomer was further purified by prep TLC (EtOAc/petroleum ether 25:75).

*For products **20a–h** and **20k***: Upon complete conversion to the *cis* and *trans* cascade products, the other reaction was directly purified by column chromatography (EtOAc/petroleum ether 15:85), isolating all diastereomeric aldehyde products together as a mixture. This diastereomeric mixture was used for the determination of the diastereomeric ratio. To 0.05 mmol of all diastereomeric aldehyde products, was added 0.5 mL $CDCl_3$. The d.r. of **24**-*cis* and **24**-*trans* were calculated by integration of the aldehyde peaks of all diastereomers of the corresponding aldehydes of **24**-*cis* and **24**-*trans* arising from the *R* and *S* enantiomers, respectively, of **7**.

The **24**-*cis*/**24**-*trans* ratio for some products had to be determined in the presence of a chiral shift reagent, (−)-Eu(hfc)$_3$ or (+)-Eu(hfc)$_3$. A solution of $CDCl_3$ (0.5 mL) and Eu(hfc)$_3$ (15 mg) was prepared. The $CDCl_3$ solution of all diastereomeric aldehyde products **24** was titrated with the Eu(hfc)$_3$ solution, adding 50 μL at a time, until the aldehyde proton peaks for the corresponding aldehydes of **24**-*cis* and **24**-*trans* were separable and could be accurately integrated to determine the **24**-*cis*/**24**-*trans* ratio. Titration with (+)-Eu(hfc)$_3$ was used for products **24b**, **24c**, **24d**, **24e**, and **24h**. Titration with (−)-Eu(hfc)$_3$ was used for products **24a** and **24g**. No chiral shift reagent was required for products **24f** and **24k**.

*For product **20i***: The d.r. and **20**-*cis*/**20**-*trans* ratio for **20i** were determined by chiral HPLC of the mixture of all diastereomers of **20i** (AD-H column, *n*-hexane/*i*PrOH 90:10, 1.0 mL min^{-1}).

*For product **20j***: The d.r. and **20**-*cis*/**20**-*trans* ratio for **20j** were determined by isolated yield of the different diastereomers of **20j** after chromatography.

Representative data for pyrans

2-((2*R*,6*R*)-6-Methyltetrahydro-2*H*-pyran-2-yl)ethanol (14a):[6] colorless oil; $[\alpha]_D^{23} = -18.6$ ($c = 2.00$ in $CHCl_3$, 90% *ee*); ^{1}H NMR (400 MHz, $CDCl_3$): $\delta = 3.80$ (m, 2H), 3.59 (m, 1H), 3.49 (m, 1H), 3.15 (bs, 1H), 1.87–1.63 (m, 3H), 1.62–1.45 (m, 3H), 1.47–1.20 (m, 2H), 1.18 ppm (d, $J = 6.2$ Hz, 3H); ^{13}C NMR (100 MHz, $CDCl_3$): $\delta = 78.9$, 74.1, 61.9, 37.9, 33.0, 31.3, 23.4, 22.2 ppm; IR (thin film, KBr): $\tilde{\nu} = 3390$, 2970, 2934, 2860, 1372, 1202, 1081, 1044, 754 cm^{-1}; HRMS (ESI): *m*/*z*: calcd for $C_8H_{16}O_2$: 144.115;, found: 144.1148 [M^+].

(2*R*,3*S*)-3-(4-Fluorophenyl)-2-((2*S*,6*S*)-6-methyltetrahydro-2*H*-pyran-2-yl)-4-nitrobutan-1-ol (15a): colorless oil; $[\alpha]_D^{23} = +17.3$ ($c = 2.00$ in $CHCl_3$, 99% *ee*); ^{1}H NMR (400 MHz, $CDCl_3$): $\delta = 7.26$–7.17 (m, 2H), 7.09–6.97 (m, 2H), 5.02 (dd, $J = 12.4$, 4.6 Hz, 1H), 4.80 (dd, $J = 12.4$, 10.9 Hz, 1H), 4.16 (d, $J = 12.6$ Hz, 1H), 4.04 (td, $J = 10.5$, 4.6 Hz, 1H), 3.64 (m, 1H), 3.27–3.13 (m, 3H), 1.80 (m, 1H), 1.66–1.50 (m, 3H), 1.38 (m, 1H), 1.30–1.10 (m, 2H), 1.19 ppm (d, $J = 6.2$ Hz, 3H); ^{13}C NMR (100 MHz, $CDCl_3$): $\delta = 163.3$, 160.9, 134.6, 134.6, 129.8, 129.7, 115.9, 115.7, 79.1, 78.7, 75.1, 59.5, 47.2, 42.4, 33.0, 29.0, 23.4, 22.2 ppm; IR (thin film, KBr): $\tilde{\nu} = 3507$, 2935, 2864, 1553, 1511, 1380, 1225, 1087, 1043, 838 cm^{-1}; the enantiomeric excess was determined by HPLC with an AS-H column (*n*-hexane/*i*PrOH 90:10), 0.5 mL min^{-1}; major enantiomer $t_R =$ 15.9 min, minor enantiomer $t_R = 18.1$ min; HRMS (ESI): *m*/*z*: calcd for $C_{16}H_{22}FNO_4$: 311.1533; found: 311.1528 [M^+].

Representative data for furans

(2*R*,3*S*)-2-((2*S*,5*S*)-5-Methyltetrahydrofuran-2-yl)-4-nitro-3-phenylbutan-1-ol (20a-*cis*): colorless amorphous solid; $[\alpha]_D^{21} = +21.2$ ($c = 2.00$ in $CHCl_3$, >99% *ee*); ^{1}H NMR (400 MHz, $CDCl_3$): $\delta = 7.40$–7.25 (m, 5H), 5.05 (dd, $J = 12.6$, 4.7 Hz, 1H), 4.94 (dd, $J = 12.6$, 10.7 Hz, 1H), 4.06 (dd, $J = 12.4$, 1.6 Hz, 1H), 3.97–3.82 (m, 3H), 3.70 (dd, $J = 12.4$, 3.7 Hz, 1H), 3.21 (brs, 1H), 1.98 (m, 1H), 1.93–1.79 (m, 2H), 1.72 (m, 1H), 1.48 (m, 1H), 1.29 ppm (d, $J = 6.1$ Hz, 3H); ^{13}C NMR (100 MHz, $CDCl_3$): $\delta =$ 138.7, 128.9, 128.2, 127.7, 81.0, 78.4, 76.0, 59.3, 46.3, 44.7, 32.8, 29.8, 21.1 ppm; IR (thin film, KBr): $\tilde{\nu} = 3455$, 2970, 1637, 1552, 1380, 702 cm^{-1}; the enantiomeric excess was determined by HPLC with an AS-H column (*n*-hexane/*i*PrOH 97:3), 0.3 mL min^{-1}; major enantiomer $t_R = 73.7$ min, minor enantiomer $t_R = 83.5$ min; HRMS (ESI): *m*/*z*: calcd for $C_{15}H_{21}NO_4$: 279.1471, found: 279.1472 [M^+].

(2*R*,3*S*)-2-((2*S*,5*R*)-5-Methyltetrahydrofuran-2-yl)-4-nitro-3-phenylbutan-1-ol (20a-*trans*): colorless amorphous solid; $[\alpha]_D^{23} = -10.7$ ($c = 0.50$ in $CHCl_3$, >99% *ee*); ^{1}H NMR (400 MHz, $CDCl_3$): $\delta = 7.40$–7.23 (m, 5H), 5.06–4.82 (m, 2H), 4.21 (m, 1H), 4.11–3.98 (m, 2H), 3.91 (m, 1H), 3.70 (m, 1H), 3.31 (brs, 1H), 2.10 (m, 1H), 1.89 (m, 2H), 1.77 (m, 1H), 1.48 (m, 1H), 1.20 ppm (d, $J = 6.1$ Hz, 3H); ^{13}C NMR (100 MHz, $CDCl_3$): $\delta =$ 138.7, 128.9, 128.2, 127.7, 80.0, 78.1, 75.8, 59.5, 46.6, 44.8, 33.5, 31.3, 21.3 ppm; IR (thin film, KBr): $\tilde{\nu} = 3441$, 2964, 1640, 1552, 1261, 1023 cm^{-1}; the enantiomeric excess was determined by HPLC with an AS-H column (*n*-hexane/*i*PrOH 90:10), 0.5 mL min^{-1}; major enantiomer $t_R = 21.7$ min, minor enantiomer $t_R = 26.7$ min; HRMS (ESI): *m*/*z*: calcd for $C_{15}H_{21}NO_4$: 279.1471; found: 279.1475 [M^+].

Full characterization of compounds of type **6b–e**, **7a–k**, **14b**, **14d**, **14e**, **15b**, **15d–f**, **18**, **20b–j**-*cis*, **20b–j**-*trans*, and **20k** as well as copies of ^{1}H NMR spectra, ^{13}C NMR spectra, and HPLC chromatograms is contained in the Supporting Information.

Acknowledgements

This work was supported by the National Science Foundation (CHE-1148295, S.E.B.M.). The authors acknowledge Dr. Cliff Soll (City University of New York) for assistance with mass spectrometry, and Dr. William Brennessel (University of Rochester) for assistance with X-ray crystallography.

[1] a) M. Marigo, T. C. Wabnitz, D. Fielenbach, K. A. Jørgensen, *Angew. Chem.* **2005**, *117*, 804–807; *Angew. Chem. Int. Ed.* **2005**, *44*, 794–797; b) Y. Hayashi, H. Gotoh, T. Hayashi, M. Shoji, *Angew. Chem.* **2005**, *117*, 4284–4287; *Angew. Chem. Int. Ed.* **2005**, *44*, 4212–4215.

[2] For a recent review of organocascade reactions, see: C. Grondal, M. Jeanty, D. Enders, *Nat. Chem.* **2010**, *2*, 167–178.

[3] For **1**-catalyzed cascade reactions involving only C–C σ bond formation, see, for example: a) H. Xie, L. Zu, H. Li, J. Wang, W. Wang, *J. Am. Chem. Soc.* **2007**, *129*, 10886–10894; b) L. Zu, H. Li, H. Xie, J. Wang, W. Jiang, Y. Tang, W. Wang, *Angew. Chem.* **2007**, *119*, 3806–3808; *Angew. Chem. Int. Ed.* **2007**, *46*, 3732–3734; *Angew. Chem.* **2007**, *119*, 3806–3808; c) I. Ibrahem, G.-L. Zhao, R. Rios, J. Vesely, H. Sundén, P. Dziedzic, A. Córdova, *Chem. Eur. J.* **2008**, *14*, 7867–7879; d) G.-L. Zhao, I. Ibrahem, P. Dziedzic, J. Sun, C. Bonneau, A. Córdova, *Chem. Eur. J.* **2008**, *14*, 10007–10011; e) J. Zhang, Z. Hu, L. Dong, Y. Xuan, C. Lou, M. Yan, *Tetrahedron: Asymmetry* **2009**, *20*, 355–361; f) M. Rueping, A. Kuenkel, F. Tato, J. W. Bats, *Angew. Chem.* **2009**, *121*, 3754–3757; *Angew. Chem. Int. Ed.* **2009**, *48*, 3699–3702; *Angew. Chem.* **2009**, *121*, 3754–3757; g) A. Ma, D. Ma, *Org. Lett.* **2010**, *12*, 3634–3637; h) S. Anwar, H.-J. Chang, K. Chen, *Org. Lett.* **2011**, *13*, 2200–2203; i) B.-C. Hong, A. A. Sadani, R. Y. Nimje, N. S. Dange, G.-H. Lee, *Synthesis* **2011**, 1887–1895.

[4] For **1**-catalyzed cascade reactions involving C-heteroatom bond formation see, for example: a) M. Marigo, J. Franzén, T. B. Poulsen, W. Zhuang, K. A. Jørgensen, *J. Am. Chem. Soc.* **2005**, *127*, 6964–6965; b) S. Brandau, E. Maerten, K. A. Jørgensen, *J. Am. Chem. Soc.* **2006**, *128*, 14986–14991; c) J. Vesely, I. Ibrahem, G.-L. Zhao, R. Rios, A. Córdova, *Angew. Chem.* **2007**, *119*, 792–795; *Angew. Chem. Int. Ed.* **2007**, *46*, 778–781; *Angew. Chem.* **2007**, *119*, 792–795; d) H. Li, L. Zu, H. Xie, J. Wang, W. Jiang, W. Wang, *Org. Lett.* **2007**, *9*, 1833–1835; e) G.-L. Zhao, J. Vesely, R. Rios, I. Ibrahem, H. Sundén, A. Córdova, *Adv. Synth. Catal.* **2008**, *350*, 237–242; f) H. Li, L. Zu, H. Xie, J. Wang, W. Wang, *Chem. Commun.* **2008**, 5636–5638; g) E. Reyes, G. Talavera, J. L. Vicario, D. Badía, L. Carrillo, *Angew. Chem.* **2009**, *121*, 5811–5814; *Angew. Chem. Int. Ed.* **2009**, *48*, 5701–5704; *Angew. Chem.* **2009**, *121*, 5811–5814; h) P. Kotame, B.-C. Hong, J.-H. Liao, *Tetrahedron Lett.* **2009**, *50*, 704–707; i) J.-Y. Bae, H.-J. Lee, S.-H. Youn, S.-H. Kwon, C.-W. Cho, *Org. Lett.* **2010**, *12*, 4352–4355.

[5] For **1**-catalyzed cascade reactions involving untethered nucleophiles and electrophiles, see: a) M. Marigo, T. Schulte, J. Franzén, K. A. Jørgensen, *J. Am. Chem. Soc.* **2005**, *127*, 15710–15711; b) H. Jiang, J. B. Nielsen, M. Nielsen, K. A. Jørgensen, *Chem. Eur. J.* **2007**, *13*, 9068–9075; c) C. Appayee, S. E. Brenner-Moyer, *Org. Lett.* **2010**, *12*, 3356–3359; d) A. Quintard, A. Alexakis, *Chem. Commun.* **2011**, *47*, 7212–7214.

[6] P. G. McGarraugh, S. E. Brenner-Moyer, *Org. Lett.* **2011**, *13*, 6460–6463 and references therein.

[7] Substrate **6e** could not be synthesized in uncyclized form, and was thus subjected to cascade reaction conditions as the corresponding racemic *cis*-tetrahydropyran.

[8] CCDC-855353 (**20a**-*cis*), -855354 (**32a**-*trans*), contain the supplementary crystallographic data for this paper. These data can be obtained free of charge from The Cambridge Crystallographic Data Centre via www.ccdc.cam.ac.uk/data_request/cif

[9] a) Gaussian 09, Revision A.1, M. J. Frisch, G. W. Trucks, H. B. Schlegel, G. E. Scuseria, M. A. Robb, J. R. Cheeseman, G. Scalmani, V. Barone, B. Mennucci, G. A. Petersson, H. Nakatsuji, M. Caricato, X. Li, H. P. Hratchian, A. F. Izmaylov, J. Bloino, G. Zheng, J. L. Sonnenberg, M. Hada, M. Ehara, K. Toyota, R. Fukuda, J. Hasegawa, M. Ishida, T. Nakajima, Y. Honda, O. Kitao, H. Nakai, T. Vreven, J. A. Montgomery, Jr., J. E. Peralta, F. Ogliaro, M. Bearpark, J. J. Heyd, E. Brothers, K. N. Kudin, V. N. Staroverov, R. Kobayashi, J. Normand, K. Raghavachari, A. Rendell, J. C. Burant, S. S. Iyengar, J. Tomasi, M. Cossi, N. Rega, N. J. Millam, M. Klene, J. E. Knox, J. B. Cross, V. Bakken, C. Adamo, J. Jaramillo, R. Gomperts, R. E. Stratmann, O. Yazyev, A. J. Austin, R. Cammi, C. Pomelli, J. W. Ochterski, R. L. Martin, K. Morokuma, V. G. Zakrzewski, G. A. Voth, P. Salvador, J. J. Dannenberg, S. Dapprich, A. D. Daniels, Ö. Farkas, J. B. Foresman, J. V. Ortiz, J. Cioslowski, D. J. Fox, Gaussian, Inc., Wallingford CT, **2009**; b) S. Grimme, *J. Comput. Chem.* **2003**, *24*, 1529–1537; c) M. Gerenkamp, S. Grimme, *Chem. Phys. Lett.* **2004**, *392*, 229–235; d) T. H. Dunning Jr., *J. Chem. Phys.* **1989**, *90*, 1007–1023.

[10] M. D. Pierce, R. C. Johnston, S. Mahapatra, H. Yang, R. G. Carter, P. H.-Y. Cheong, *J. Am. Chem. Soc.*, DOI 10.1021/ja3018219).

[11] Side views of all transition structures in Figure 2 can be found in the Supporting Information.

[12] a) P. H.-Y. Cheong, C. Y. Legault, J. M. Um, N. Çelebi-Ölçüm, K. N. Houk, *Chem. Rev.* **2011**, *111*, 5042–5137; b) P. Dinér, A. Kjærsgaard, M. A. Lie, K. A. Jørgensen, *Chem. Eur. J.* **2008**, *14*, 122–127.

[13] Nonclassical hydrogen bonding interactions have been invoked in stereochemical models of other organocatalytic reactions, for example: a) S. Bahmanyar, K. N. Houk, *J. Am. Chem. Soc.* **2001**, *123*, 12911–12912; b) C. E. Cannizzaro, K. N. Houk, *J. Am. Chem. Soc.* **2002**, *124*, 7163–7169; c) S. Bahmanyar, K. N. Houk, H. J. Martin, B. List, *J. Am. Chem. Soc.* **2003**, *125*, 2475–2479; d) C. Allemann, R. Gordillo, F. R. Clemente, P. H.-Y. Cheong, K. N. Houk, *Acc. Chem. Res.* **2004**, *37*, 558–569; e) P. H.-Y. Cheong, K. N. Houk, *Synthesis* **2005**, 1533–1537; f) H. Yang, S. Mahapatra, P. H.-Y. Cheong, R. G. J. Carter, *J. Org. Chem.* **2010**, *75*, 7279–7290.

[14] a) J. Burés, A. Armstrong, D. G. Blackmond, *J. Am. Chem. Soc.* **2011**, *133*, 8822–8825; b) Blackmond and Armstrong published an elaboration of this and other studies after submission of our manuscript: J. Burés, A. Armstrong, D. G. Blackmond, *J. Am. Chem. Soc.* **2012**, *134*, 6741—6750.

Received: December 23, 2011
Revised: March 27, 2012
Published online: ■■ ▮▮, 0000

Organocatalysis

P. G. McGarraugh, R. C. Johnston, A. Martínez-Muñoz, P. H.-Y. Cheong, S. E. Brenner-Moyer** ..... ▮▮▮▮–▮▮▮▮

Organocatalytic Kinetic Resolution Cascade Reactions: New Mechanistic and Stereochemical Manifold in Diphenyl Prolinol Silyl Ether Catalysis

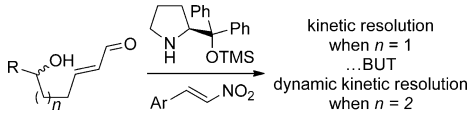

A new resolution for 2012: A cascade reaction generating enantiopure, highly functionalized tetrahydropyrans and -furans in a one-pot reaction is described. The stereochemical outcome of this cascade reaction is unprecedented. The cascade reaction also proceeds by an unprecedented mechanism, in which a kinetic resolution or dynamic kinetic resolution of the β-stereocenter occurs, mediated by the enamine-catalyzed intermolecular reaction (see scheme).